Human DNA Polymerase α Uses a Combination of Positive and Negative Selectivity To Polymerize Purine dNTPs with High Fidelity†

Jeff Beckman,‡ Kristi Kincaid,‡ Michal Hocek,§ Thomas Spratt,|| Joachim Engels,⊥ Richard Cosstick,@ and Robert D. Kuchta*,‡

Department of Chemistry and Biochemistry, University of Colorado, Boulder, Colorado 80309-0215, Centre for New Antivirals and Antineoplastics, Institute of Organic Chemistry and Biochemistry, Academy of Sciences of the Czech Republic, CZ-16610 Prague 6, Czech Republic, Department of Biochemistry and Molecular Biology, Penn State College of Medicine, 500 University Drive, Hershey, Pennsylvania 17033, Institut für Organische Chemie, Johann Wolfgang Goethe Universität, Marie Curie Strasse 11, D-60439 Frankfurt am Main, Germany, and Department of Chemistry, University of Liverpool, Crown Street, Liverpool L69 3BX, U.K.

Received June 22, 2006; Revised Manuscript Received November 2, 2006

ABSTRACT: DNA polymerases accurately replicate DNA by incorporating mostly correct dNTPs opposite any given template base. We have identified the chemical features of purine dNTPs that human pol α uses to discriminate between right and wrong dNTPs. Removing N-3 from guanine and adenine, two high-fidelity bases, significantly lowers fidelity. Analogously, adding the equivalent of N-3 to low-fidelity benzimidazole-derived bases (i.e., bases that pol α rapidly incorporates opposite all four natural bases) and to generate 1-deazapurines significantly strengthens the ability of pol α to identify the resulting 1-deazapurines as wrong. Adding the equivalent of the purine N-1 to benzimidazole or to 1-deazapurines significantly decreases the rate at which pol α polymerizes the resulting bases opposite A, C, and G while simultaneously enhancing polymerization opposite T. Conversely, adding the equivalent of adenine's C-6 exocyclic amine (N-6) to 1- and 3-deazapurines also enhances polymerization opposite T but does not significantly decrease polymerization opposite A, C, and G. Importantly, if the newly inserted bases lack N-1 and N-6, pol α does not efficiently polymerize the next correct dNTP, whereas if it lacks N-3, one additional nucleotide is added and then chain termination ensues. These data indicate that pol α uses two orthogonal screens to maximize its fidelity. During dNTP polymerization, it uses a combination of negative (N-1 and N-3) and positive (N-1 and N-6) selectivity to differentiate between right and wrong dNTPs, while the shape of the base pair is essentially irrelevant. Then, to determine whether to add further dNTPs onto the just added nucleotide, pol α appears to monitor the shape of the base pair at the primer 3′-terminus. The biological implications of these results are discussed.

A hallmark feature of cells is their ability to accurately replicate DNA. This is thought to result from a three-stage process. First, replicative DNA polymerases rarely incorporate the wrong dNTP.[1] Second, the polymerase proofreads the newly incorporated nucleotide. If the just added nucleotide is correct, polymerization continues at a rapid rate. However, if the nucleotide is incorrect, the rate of addition of the next correct dNTP becomes very slow, allowing the polymerase to either excise the error itself or dissociate and allow a separate exonuclease to perform the task. Finally, if the polymerase incorporates an incorrect dNTP and follows that by polymerizing additional dNTPs, postreplicative repair enzymes can remove the incorrect nucleotide and fill the

† This work was supported by grants to R.D.K. from the National Institutes of Health (GM54194 and TW007372-01) and the Army Research Office (W911NF-05-1-0172), to M.H. from the Ministry of Education of the Czech Republic (Centre of Biomolecules and Complex Molecular Systems, LC 512), and to J.E. from the Deutsche Forschungsgemeinschaft (SFB 579).

* To whom correspondence should be addressed. E-mail: kuchta@colorado.edu. Phone: (303) 492-7027. Fax: (303) 492-5894.

‡ University of Colorado.

§ Academy of Sciences of the Czech Republic.

|| Penn State College of Medicine.

⊥ Johann Wolfgang Goethe Universität.

@ University of Liverpool.

[1] Abbreviations: A, adenine; 4AB, 4-aminobenzimidazole; B, benzimidazole; 1DA, 1-deazaadenine; Q, 1-deaza-6-methylpurine; 1DP, 1-deazapurine; 3DP, 3-deazapurine; Z, 4-methylbenzimidazole; 6MP, 6-methylpurine; P, purine; $4F_3B$, 4-trifluoromethylbenzimidazole; $6F_3P$, 6-trifluoromethylpurine; d1DATP, 9-β-D-2′-deoxyribofuranosyl(1-deazaadenine)-5′-triphosphate; d1DPTP, 9-β-D-2′-deoxyribofuranosyl(1-deazapurine)-5′-triphosphate; d3DATP, 9-β-D-2′-deoxyribofuranosyl(3-deazaadenine)-5′-triphosphate; d3DGTP, 9-β-D-2′-deoxyribofuranosyl(3-deazaguanine)-5′-triphosphate; d3DPTP, 9-β-D-2′-deoxyribofuranosyl(3-deazapurine)-5′-triphosphate; d4ABTP, 1-β-D-2′-deoxyribofuranosyl(4-aminobenzimidazole)-5′-triphosphate; $d4F_3BTP$, 1-β-D-2′-deoxyribofuranosyl(4-trifluoromethylbenzimidazole)-5′-triphosphate; $d6F_3PTP$, 9-β-D-2′-deoxyribofuranosyl(6-trifluoromethylpurine)-5′-triphosphate; d6MPTP, 9-β-D-2′-deoxyribofuranosyl(6-methylpurine)-5′-triphosphate; dBTP, 1-β-D-2′-deoxyribofuranosyl(benzimidazole)-5′-triphosphate; dNTP, natural 2′-deoxy-5′-triphosphate; dPTP, 9-β-D-2′-deoxyribofuranosyl(purine)-5′-triphosphate; dQTP, 9-β-D-2′-deoxyribofuranosyl(1-deaza-6-methylpurine)-5′-triphosphate; dZTP, 1-β-D-2′-deoxyribofuranosyl(4-methylbenzimidazole)-5′-triphosphate; ESI, electrospray ionization; MALDI, matrix-assisted laser desorption ionization; NOE, nuclear Overhauser effect; pol α, DNA polymerase α; SD, standard deviation; THAP, 2′,4′,6′-trihydroxyacetophenone; Tris-HCl, tris(hydroxymethyl)-aminomethane-hydrochloric acid.

10.1021/bi061243s CCC: $37.00
Published on Web 12/16/2006

resulting gap. Overall, this results in an error frequency of ca. 10^{-9} error per nucleotide inserted (*1*).

Replicative DNA polymerases, e.g., DNA polymerase α (pol α), exhibit error frequencies of $10^{-3}-10^{-6}$ errors per nucleotide inserted (*2*, *3*). Over the past few decades, multiple theories to account for the ability of these polymerases to accurately differentiate between right and wrong dNTPs have been proposed. Originally, Watson and Crick proposed that replication fidelity is due to the self-complementarity of the bases via the two hydrogen bonds between A and T and the three between G and C (*4*, *5*). Although recent studies have shown that two low-fidelity RNA polymerases, human and herpes DNA primase, most likely incorporate correct NTPs on the basis of these hydrogen bonds (*6*, *7*), many DNA polymerases clearly do not use this mechanism. In a series of pioneering studies, Kool and co-workers showed that some DNA polymerases (for example, Klenow fragment) will generate a base pair between analogues containing the bases 2,4-difluorotoluene, a thymine isostere, and 4-methylbenzimidazole, an adenine isostere. These studies clearly indicated that some polymerases do not require formation of Watson−Crick hydrogen bonds for rapid dNTP polymerization and suggest that the shape of the incipient base pair may help some polymerases discriminate between right and wrong dNTPs (*8*−*10*).

However, recent studies using human pol α, a family-B polymerase, showed that this enzyme does not require either formation of hydrogen bonds or a correctly shaped incipient base pair to rapidly polymerize a dNTP (*11*, *12*). Pol α polymerizes dNTP analogues containing bases such as benzimidazole, 4-methoxybenzimidazole, and 5,6-dinitrobenzimidazole opposite all four natural template bases with remarkable efficiency, incorporating them at rates approaching those for a correct, natural dNTP, and orders of magnitude faster than an incorrect, natural dNTP (V_{max}/K_M). While we do not know the shape of the base pairs formed between these analogues and, for example, adenine or guanine, it clearly must be quite different from a canonical base pair. Thus, a correctly shaped base pair is not essential for dNTP polymerization by pol α. These studies also indicated that the rapid polymerization of these unnatural, low-fidelity bases did not result from their relatively high hydrophobicity (*11*).

Importantly, after pol α incorporates these low-fidelity nucleotides, it does not efficiently incorporate the next correct dNTP. These data suggest that pol α uses very different mechanisms to choose whether to polymerize a dNTP versus when to rapidly add further dNTPs onto a newly polymerized nucleotide and have led to the idea that pol α uses two orthogonal screens to ensure fidelity. The first screen occurs during dNTP polymerization where pol α uses one set of parameters to decide whether to polymerize the dNTP. The second screen occurs during addition of the next correct dNTP onto a primer terminus, and pol α now uses a different set of parameters.

To better understand how pol α discriminates between right and wrong dNTPs, we posed two questions. What chemical features have to be added to an unnatural, low-fidelity base (e.g., benzimidazole or 4-methylbenzimidazole) to convert it into a high-fidelity base (e.g., adenine), and what chemical features have to be removed from a high-fidelity base to convert it into a low-fidelity base? Pol α uses N-1 and N-3 of a purine to specifically prevent misincorporation of a purine dNTP, whereas N-1 and adenine's exocyclic amine at C-6 specifically enhance the correct incorporation of the dNTP. In contrast, the shape of the base pair at the primer 3′-terminus appears to primarily dictate the rate at which pol α polymerizes additional dNTPs.

EXPERIMENTAL PROCEDURES

Materials. All reagents were of the highest quality commercially available. Unlabeled dNTPs were purchased from Sigma and radiolabeled dNTPs from New England Nuclear. Synthetic oligonucleotides were purchased from Oligos, Etc., or BioSearch, and their concentrations were determined spectrally. Human pol α (four-subunit complex) was expressed and purified as previously described (*13*). 9-(2-Deoxy-β-D-*erythro*-pentofuranosyl)purine was purchased from Berry and Associates (Ann Arbor, MI). 9-(2-Deoxy-β-D-*erythro*-pentofuranosyl)-1-deazapurine was synthesized as previously described (*14*). 9-(2-Deoxy-β-D-*erythro*-pentofuranosyl)-6-chloro-3-deazapurine (Berry and Associates) was hydrogenated to 9-(2-deoxy-β-D-*erythro*-pentofuranosyl)-3-deazapurine as previously described (*15*). 1-β-D-2′-Deoxyribofuranosyl(4-trifluoromethylbenzimidazole)-5′-triphosphate (d4F_3BTP), 1-β-D-2′-deoxyribofuranosyl(4-methylbenzimidazole)-5′-triphosphate (dZTP), 9-β-D-2′-deoxyribofuranosyl(1-deaza-6-methylpurine)-5′-triphosphate (dQTP), 9-β-D-2′-deoxyribofuranosyl(3-deazaadenine)-5′-triphosphate (d3DATP), and 9-β-D-2′-deoxyribofuranosyl(3-deazaguanine)-5′-triphosphate (d3DGTP) were synthesized as previously described (*9*, *11*, *16*−*19*). Triphosphorylation of 9-(2-deoxy-β-D-*erythro*-pentofuranosyl)-1-deazaadenine to 9-β-D-2′-deoxyribofuranosyl(1-deazaadenine)-5′-triphosphate (d1DATP) was performed by Sierra Bioresearch (Tucson, AZ).

Chemical Methods. Unless otherwise noted, materials from commercial sources were used without further purification. Chromatographic separations were performed on grade 62, 60−200 mesh (Aldrich). Thin layer chromatography was performed on aluminum silica gel plates (Silica Gel 60 F_{254}, EMD Chemicals Inc.). ^{1}H NMR was performed on either Inova 400 MHz or Varian 500 MHz instruments and internally referenced to a trace impurity (H_2O). ^{31}P NMR was performed on the Inova 400 MHz instrument and referenced using 85% phosphoric acid in a capillary tube inserted into the sample. All chemical shifts are reported in parts per million (δ) unless otherwise noted.

Synthesis of Nucleosides. Synthesis was achieved by glycosylating a purine (analogue) with 1-(α)-chloro-3,5-di-*O*-(*p*-toluoyl)-2-deoxy-D-ribose (Berry and Associates) using the procedure of Kazimierczuk and colleagues (*20*). Briefly, the purine/purine analogue was added to enough dry MeCN to fully dissolve it (an approximately 20 mM solution is typical). NaH (60% in oil, 1 equiv) was then added and the mixture allowed to equilibrate at room temperature for 30 min. This mixture was cooled on ice and the 1-α-chloro-3,5-di-*O*-(*p*-toluoyl)-2-deoxy-D-ribose (1 equiv) added. After approximately 3 h on ice, the slurry was filtered, dried under vacuum, and then silica purified using a 70:30 ethyl acetate (EtOAc)/hexanes mixture for benzimidazole nucleosides and a 95:5 methylene chloride (CH_2Cl_2)/MeOH mixture for

1-deazapurine nucleosides. Yields were generally between 40 and 70%, depending on the percentage of β to α anomers and regioisomers that formed during coupling. Protected nucleosides were deprotected by dissolving them first in MeOH followed by addition of sodium methoxide (NaOMe) (approximately 10 mM starting material in MeOH was typical; 2 equiv of NaOMe). After 2−3 h, the reaction was quenched using excess ammonium chloride (NH_4Cl), and the mixture was filtered and dried under vacuum. A small amount of ddH_2O (10 mL) was added to dissolve the solids, and the product was extracted twice into EtOAc (2 × 100 mL). The organic layer was dried using magnesium sulfate ($MgSO_4$) and filtered, and the nucleoside was purified using silica flash chromatography (9:1 CH_2Cl_2/MeOH mixture) followed by HPLC purification (Beckman semipreparative reverse phase column, 0 to 60% MeCN in H_2O). Typically yields were between 80 and 90%. Using NOE (GOESY) NMR, benzimidazole bases were assigned as the correct regioisomer by observing the interaction between C7 of the base and anomeric H-1′ of the 2′-deoxyribose. For 1-deazapurines, the lack of interaction between the anomeric proton and the base was observed.

Synthesis of 9-(2-Deoxy-β-D-erythro-pentofuranosyl)-1-deazaadenine. 1-Deazaadenine [130 mg (1 mmol), synthesized as previously described (*21*, *22*)] was protected at its exocyclic amine to form the acetamide by dissolving it into 20 mL of a pyridine/acetic anhydride solution (3:1) and heating to 70 °C for 6 h. After cooling to room temperature, it was dried under vacuum, triturated into 150 mL of EtOAc, filtered, and then vacuum-dried. The 6-acetamide-1-deazaadenine was purified as a yellow solid in 70% yield using silica flash chromatography (9:1 CH_2Cl_2/MeOH mixture). ^{1}H NMR (400 MHz, d_4-methanol): δ 8.75 (1H, s, C_2H), 8.32 (1H, d, J_{gem} = 6.0 Hz, ArH), 8.21 (1H, d, J_{gem} = 6.0 Hz, ArH), 2.26 (3H, s, CH_3). 6-Acetamide-1-deazaadenine (90 mg, 500 μmol) was dissolved into 20 mL of dry MeCN (25 mM solution), and the protected nucleoside was generated in 50% yield using the procedure described previously. The protected nucleoside (50 mg, 95 μmol) was dissolved in 15 mL of MeOH saturated with ammonia (saturated at 0 °C; 6 mM solution), allowed to be deprotected overnight at room temperature, dried under vacuum, and then purified by silica flash chromatography (9:1 CH_2Cl_2/MeOH mixture) to produce 9-(2-deoxy-β-D-*erythro*-pentofuranosyl)-6-acetamide-1-deazapurine in 90% yield. ^{1}H NMR (500 MHz, d_4-methanol): δ 8.45 (1H, s, C_2H), 8.19 (1H, d, J_{gem} = 7.0 Hz, ArH), 8.14 (1H, d, J_{gem} = 7.0 Hz, ArH), 6.50 (1H, dd, $J_{1',2'}$ = 8.0, 10.5 Hz, H-1′), 4.57 (1H, m, H-3′), 4.06 (1H, m, H-4′), 3.70−3.84 (2H, m, H-5′), 2.85 (1H, m, H-2′b), 2.37 (1H, m, H-2′a), 2.24 (3H, s, CH_3). Conversion to 9-(2-deoxy-β-D-*erythro*-pentofuranosyl)-1-deazaadenine in 90% yield was conducted by dissolving 40 mg of 9-(2-deoxy-β-D-*erythro*-pentofuranosyl)-6-acetamide-1-deazapurine in MeOH (a 10 mM solution), adding excess NaOMe (approximately 3 equiv), refluxing the mixture for 6 h followed by addition of excess NH_4Cl, and letting it stir for an additional 1 h. After being filtered and vacuum-dried, the product was purified by flash chromatography (92:8 CH_2Cl_2/MeOH mixture). ^{1}H NMR (400 MHz, d_4-methanol): δ 8.22 (1H, s, C_2H), 7.81 (1H, d, J_{gem} = 6.0 Hz, ArH), 6.46 (1H, d, J_{gem} = 6.0 Hz, ArH), 6.40 (1H, dd, $J_{1',2'}$ = 6.0, 8.8 Hz, H-1′), 4.54 (1H, m, H-3′), 4.05 (1H, m, H-4′), 3.69−3.84 (2H, m, H-5′), 2.84 (1H, m, H-2′b), 2.33 (1H, m, H-2′a). MS (ESI+): 251.1134 ($[M + H]^+$ calcd 251.1138).

Synthesis of 9-(2-Deoxy-β-D-erythro-pentofuranosyl)-6-(trifluoromethyl)purine. Synthesis was performed using a modification of an established method (*23*, *24*). A mixture of 9-[3,5-bis-*O*-(4-methylbenzoyl)-2-deoxy-β-D-*erythro*-pentofuranosyl]-6-iodopurine (300 mg, 0.5 mmol) (trifluoromethyl)trimethylsilane (CF_3SiMe_3) (206 μL, 1.4 mmol), potassium fluoride (KF) (82 mg, 1.4 mmol), copper iodide (CuI) (150 mg, 0.8 mmol), dimethylformamide (DMF) (1 mL), and 1-methyl-2-pyrrolidinone (NMP) (1 mL) was stirred at 60 °C for 24 h. After cooling to room temperature, the solvents were evaporated under low pressure, and the residue was chromatographed on a silica gel column in a 1:4 EtOAc/hexanes mixture to 1:1 to give oily 9-[3,5-bis-*O*-(4-methylbenzoyl)-2-deoxy-β-D-*erythro*-pentofuranosyl]-6-trifluoromethylpurine (140 mg, 58%). This intermediate was deprotected by being treated with 50 mL of 0.2 mM NaOMe in MeOH at room temperature for 12 h. The solvent was evaporated and the residue crystallized from a MeOH/toluene/heptane mixture to give the crystalline title compound (78 mg, 89% yield of deprotection, 51% overall yield). All analytical and spectral data were identical to those of an authentic sample (*23*).

Synthesis of 9-(2-Deoxy-β-D-erythro-pentofuranosyl)-6-methylpurine. This compound was synthesized by a modification of an established procedure (*25*−*27*). Methylmagnesium chloride (MeMgCl) [2 mL of a 3 M solution in tetrahydrofuran (THF)] was added dropwise to a solution of 9-[3,5-bis-*O*-(4-methylbenzoyl)-2-deoxy-β-D-*erythro*-pentofuranosyl]-6-chloropurine (848 mg, 1.67 mmol) and iron(III) acetylacetonate [$Fe(acac)_3$] (103 mg, 0.29 mmol) in a mixture of 1-methyl-2-pyrrolidinone (NMP, 1 mL) and THF (10 mL) at room temperature under an argon atmosphere. The mixture was then stirred for 2 h, poured onto a mixture of crushed ice (100 mL) and NH_4Cl (1 g), and extracted into EtOAc (2 × 100 mL). The combined organic layers were dried over $MgSO_4$ and evaporated. The residue was chromatographed on a silica gel column (100 g) in a 1:4 EtOAc/hexanes mixture to 1:1 to give oily 9-[3,5-bis-*O*-(4-methylbenzoyl)-2-deoxy-β-D-*erythro*-pentofuranosyl]-6-methylpurine (550 mg, 77%). This intermediate was deprotected by being treated with 50 mL of 0.2 mM NaOMe in MeOH at room temperature for 12 h. The solvent was evaporated and the residue crystallized from a MeOH/toluene/heptane mixture to give the crystalline title compound (295 mg, 98% yield of deprotection, 75% overall yield) as white crystals. Mp: 153−155 °C [mp reported to be 161 °C (*25*, *26*)]. ^{1}H NMR (400 MHz, DMSO-d_6): δ 8.77 (s, 1H, H-2), 8.73 (s, 1H, H-8), 6.45 (t, 1H, $J_{1',2'}$ = 7.2, 6.3 Hz, H-1′), 5.60 (br, 1H, OH-3′), 5.20 (br, 1H, OH-5′), 4.45 (m, 1H, H-3′), 3.88 (m, 1H, H-4′), 3.62 (dd, 1H, J_{gem} = 11.8 Hz, $J_{5'a,4'}$ = 4.6 Hz, H-5′a), 3.53 (dd, 1H, J_{gem} = 11.8 Hz, $J_{5'b,4'}$ = 4.5 Hz, H-5′b), 2.76 (ddd, 1H, J_{gem} = 13.3 Hz, $J_{2'a,1'}$ = 7.2 Hz, $J_{2'a,3'}$ = 6.0 Hz, H-2′a), 2.71 (s, 3H, CH_3), 2.33 (ddd, 1H, J_{gem} = 13.3 Hz, $J_{2'b,1'}$ = 6.3 Hz, $J_{2'b,3'}$ = 3.7 Hz, H-2′b). MS (MALDI+): 251 ($[M + H]^+$ calcd 251).

Synthesis of 2′-Deoxyribofuranoside Triphosphates. Phosphorylation was achieved via the protocol of Ludwig using phosphorus oxychloride and tributylammonium pyrophosphate (*19*). Briefly, nucleosides were dried under vacuum and then added to cold, freshly distilled $PO(OMe)_3$ (ap-

proximately 1 mL of a 40 mM solution) before addition of 1.5 equiv of $POCl_3$ (99.999%, Aldrich). After being stirred on ice overnight, the solution was warmed to room temperature, and 5 equiv of tributylammonium pyrophosphate (anhydrous, Sigma) as a 1 M solution in dry DMF was added and allowed to react for approximately 30 min. Triethylammonium bicarbonate (TEAB, 5 mL of a 0.1 M solution) was added to quench the reaction. The resulting product solution was then diluted to 200 mL and added directly to a TEAB-equilibrated ion-exchange column (Sephadex-DEAE A-25, Aldrich) and eluted using a 0 to 1 M TEAB gradient. Fractions were individually spotted on a MALDI plate with 2,4,6-trihydroxyacetophenone (THAP) as the matrix, and triphosphate fractions were identified by their MALDI$^-$ peak (negative ion mode). Triphosphate fractions were collected, dried (with the aid of EtOH to help remove triethylamine), and purified by HPLC using a 50 min gradient from 0 to 60% MeCN in 20 mM triethylammonium acetate (TEAA, pH 7.5). For the analogue triphosphates containing the bases purine, 6-methylpurine, and 6-trifluoromethylpurine, the solvent contained 100 mM TEAA.

Synthesis of 1-β-D-2′-Deoxyribofuranosyl(4-aminobenzimidazole)-5′-triphosphate (d4ABTP). 1,2-Diamino-3-nitrobenzene (400 mg, 3 mmol, Aldrich) was dissolved in 20 mL of 97% formic acid (a 100 mM solution) and refluxed at 110 °C overnight. The dark solution was filtered through Celite and dried under vacuum, dissolved in 40 mL of water, and then extracted with EtOAc (3 × 150 mL). The combined organic layers were dried using $MgSO_4$ and reduced to dryness under vacuum (70% yield, used without further purification). ^{1}H NMR (300 MHz, DMSO-d_6): δ 8.44 (1H, s, C_2H), 8.15 (2H, br d, J_{gem} = 4.8 Hz, ArH), 7.40 (1H, dd, $J_{gem1,2}$ = 4.8 Hz, ArH). 4-Nitrobenzimidazole was converted into the nucleoside and nucleoside triphosphates as described earlier. ^{1}H NMR (500 MHz, acetone-d_6) for 1-(2-deoxy-β-D-*erythro*-pentofuranosyl)-4-nitrobenzimidazole: δ 8.63 (1H, s, C_2H), 8.17 (1H, d, J_{gem} = 8.5 Hz, J_{vic} = 0.5 Hz, ArH), 8.02 (1H, d, J_{gem} = 8.0 Hz, J_{vic} = 0.5 Hz, ArH), 7.44 (1H, dd, $J_{gem1,2}$ = 8.0 Hz, ArH), 6.49 (1H, dd, $J_{1',2'}$ = 6.5, 7.0 Hz, H-1′), 4.64 (1H, m, H-3′), 4.03 (1H, m, H-4′), 3.76 (2H, m, H-5′), 2.72 (1H, m, H-2′b), 2.51 (1H, m, H-2′a). MS (MALDI+): 302 ([M + Na]$^+$ calcd 302). ^{31}P NMR (400 MHz, D_2O) for 1-β-D-2′-deoxyribofuranosyl(4-nitrobenzimidazole)-5′-triphosphate (d4NO_2BTP): δ −10.1 (br d, γ-P), −10.8 (br d, α-P), −22.5 (br m, β-P). MS (MALDI-): 518 ([M − H]$^-$ calcd 518). To 500 μL of 15 mM d4NO_2-BTP was added 15 mg of 10% palladium on carbon (Pd/C). While the mixture was being stirred, 1 atm (balloon) of H_2 was applied for 3 h at room temperature to effect complete conversion to 1-β-D-2′-deoxyribofuranosyl(4-aminobenzimidazole)-5′-triphosphate (d4ABTP). ^{31}P NMR (400 MHz, D_2O): δ −4.66 (br, γ-P), −9.76 (br, α-P), −18.3 (br, β-P). MS (MALDI-): 488 ([M − H]$^-$ calcd 488).

^{31}P NMR (400 MHz, D_2O) for 9-β-D-2′-deoxyribofuranosyl(1-deazapurine)-5′-triphosphate (d1DPTP): δ −8.52 (br, γ-P), 10.5 (d, α-P), 21.8 (br, β-P). MS (MALDI-): 474 ([M − H]$^-$ calcd 474).

^{31}P NMR (400 MHz, D_2O) for 9-β-D-2′-deoxyribofuranosyl(3-deazapurine)-5′-triphosphate (d3DPTP): δ −7.05 (d, γ-P), −10.1 (d, α-P), −20.6 (dd, β-P). MS (MALDI-): 474 ([M − H]$^-$ calcd 474).

^{31}P NMR (400 MHz, D_2O) for 9-β-D-2′-deoxyribofuranosyl(purine)-5′-triphosphate (dPTP): δ −9.91 (d, γ-P), −10.6 (d, α-P), −22.3 (t, β-P). MS (MALDI-): 475 ([M − H]$^-$ calcd 475).

^{31}P NMR (400 MHz, D_2O) for 9-β-D-2′-deoxyribofuranosyl(6-methylpurine)-5′-triphosphate (d6MPTP): δ −5.05 (br, γ-P), −9.96 (d, α-P), −19.5 (br, β-P). MS (MALDI-): 489 ([M − H]$^-$ calcd 489).

^{31}P NMR (400 MHz, D_2O) for 9-β-D-2′-deoxyribofuranosyl(6-trifluoromethylpurine)-5′-triphosphate (d6F_3PTP): δ −5.99 (br, γ-P), −10.1 (br, α-P), −19.6 (br, β-P). MS (MALDI-): 543 ([M − H]$^-$ calcd 543).

^{31}P NMR (400 MHz, D_2O) for 9-β-D-2′-deoxyribofuranosyl(1-deazaadenine)-5′-triphosphate (d1DATP): δ −9.29 (br, γ-P), −10.6 (d, α-P), −22.0 (br, β-P). MS (MALDI-): 489 ([M − H]$^-$ calcd 489).

5′-End Labeling of Primers and Annealing of Primer−Template Motifs. DNA primers were HPLC purified, labeled with ^{32}P at the 5′-end using [γ-^{32}P]ATP and polynucleotide kinase, and annealed to each of the four templates as previously described (*28*, *29*).

Polymerization Assays. Steady-state assays contained 1 μM 5′-[^{32}P]primer−template, 10 mM $MgCl_2$, 50 mM Tris-HCl (pH 7.6), 1 mM dithiothreitol, 0.05 mg/mL bovine serum albumin, and various concentrations of natural or analogue dNTPs in a total volume of 5 or 10 μL. Reactions were initiated by adding enzyme, mixtures incubated at 37 °C, and reactions quenched by adding 5 μL of gel loading buffer (90% formamide in 1× Tris/borate/EDTA buffer, 0.05% xylene cyanol, and bromophenol blue). Products were separated by denaturing gel electrophoresis (20% acrylamide and 8 M urea) and analyzed by phosphorimagery (Molecular Dynamics). Kinetic parameters were determined by fitting the data to the Michaelis−Menten equation using KaleidaGraph. All rates were normalized to the same final enzyme concentration (2 nM).

Polymerase Read-Through Assays. The ability of pol α to elongate past a newly incorporated analogue was determined under steady-state conditions. Six analogue dNTPs (d3DATP, dPTP, d6MPTP, d3DPTP, d1DPTP, and d4ABTP; see Figure 1) and dATP were each incorporated separately by Klenow fragment onto the 3′-end of a primer−template motif (DNA_T; see Figure 2) to make a series of "primerX−templates". Depending upon the ability of Klenow fragment to polymerize the analogue, each reaction mixture was incubated for 5−50 min and contained 5−25 units of exo$^-$ Klenow fragment (New England Biolabs), 100−1000 μM dNTP analogue, 10 mM $MgCl_2$, 50 mM Tris-HCl (pH 7.6), 1 mM dithiothreitol, 0.05 mg/mL bovine serum albumin, and 60 μM DNA_T. Each of these "primerX's" was gel purified under denaturing conditions (8 M urea and 20% acrylamide), extracted overnight into water, and subsequently reannealed to DNA_T. An eighth primerX−template motif, containing 1-deazadA at the primer terminus, was generated using pol α under analogous conditions.

Using these primerX−templates, we measured the extent of incorporation of the next-correct dNTP (dTTP) and the subsequent, second-correct dNTP (dATP) under assay conditions similar to those described above. For the latter, a "running-start"-type analysis was employed (*30*); we varied the concentration of dATP while keeping the concentration of dTTP static (100 μM). Kinetic parameters were deter-

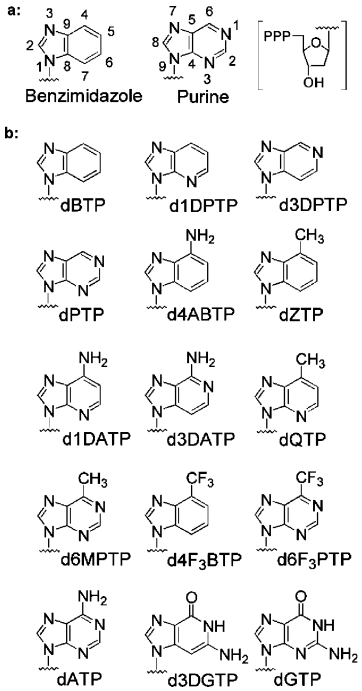

FIGURE 1: Structures, names, and numbering schemes of the dNTPs that are discussed. (a) Generic structure of benzimidazole and purine 2′-deoxyribofuranosyl-5′-triphosphates, including numbering schemes for the two aromatic systems. (b) Analogue and natural dNTPs that are discussed.

DNA_A 5′-TCCATATCACAT
3′-AGGTATAGTGTA**A**TTCTTATCATCT

DNA_T 5′-TCCATATCACAT
3′-AGGTATAGTGTA**T**TCTTATCATCT

DNA_C 5′-TCCATATCACAT
3′-AGGTATAGTGTA**C**TCTTATCATCT

DNA_G 5′-TCCATATCACAT
3′-AGGTATAGTGTA**G**TCTTATCATCT

FIGURE 2: Four primer−template sequences used in this study to determine rates of incorporation by human pol α. The template base immediately opposite the incoming nucleotide is in bold.

mined by fitting the data to the Michaelis−Menten equation using KaleidaGraph.

Determination of LogP. We measured logP using 1-octanol as the organic phase (*31*). The free bases were dissolved in 1-octanol saturated with water or vice versa, depending on which solvent dissolved the solute best, and their extinction coefficients were determined. Aided by UV spectroscopy, we determined the volume ratio of 1-octanol to water required to separate equal amounts of solute into each phase to calculate the value of P. For each free base, P values were calculated at three different solute concentrations (a 10-fold range) and an average was taken before calculating the final logP value. Each base was analyzed under neutral conditions (using 0.1 N NaOH or 0.1 N HCl). Observed wavelengths for each base (same as λ_{max}) are as follows: benzimidazole (B), 244 nm; 1-deaza-6-methylpurine (Q), 280 nm; 4-methylbenzimidazole (Z), 248 nm; 1-deazapurine (1DP), 282 nm; 3-deazapurine (3DP), 264 nm; 6-methylpurine (6MP), 262 nm; purine (P), 264 nm; 4-aminobenzimidazole (4AB), 262 nm; 6-trifluoromethylpurine ($6F_3P$), 273 nm; 4-trifluoromethylbenzimidazole ($4F_3B$), 252 nm; adenine (A), 260 nm; 1-deazaadenine (1DA), 266 nm.

Table 1: Kinetic Parameters for Correct Incorporation of Natural dNTPs by Human Pol α[a]

dNTP	DNA_N	V_{max}	K_M	V_{max}/K_M
dTTP	DNA_A	3.6 (1.4)	2.7 (1.4)	1.3
dATP	DNA_T	10 (1.4)	5.9 (2.5)	1.7
dGTP	DNA_C	8.2 (3.1)	1.4 (0.5)	5.9
dCTP	DNA_G	5.5 (1.5)	6.6 (2.0)	0.8

[a] Assays were performed and analyzed as described in Experimental Procedures. The units for V_{max} and K_M are % of primer elongated min^{-1} and μM^{-1}, respectively. The units for V_{max}/K_M are % elongated μM^{-1} min^{-1}.

RESULTS

Previous studies showed that pol α readily polymerizes dNTP analogues whose base size, shape, and chemical features do not closely resemble those of a canonical base (*11*, *12*). These dNTP analogues, which will be termed low-fidelity dNTPs, contain bases such as benzimidazole, 4-methylbenzimidazole, and 5,6-dinitrobenzimidazole and are readily polymerized opposite all four natural bases. To discover why pol α incorporates these low-fidelity dNTP analogues so efficiently, we asked two questions. (i) What features have to be removed from a high-fidelity base such as adenine (or guanine) to convert it into a low-fidelity base [i.e., it is more readily misincorporated opposite A, C, and G (or T, A, and G)]? (ii) What features have to be added to a low-fidelity base to convert it into a high-fidelity base (i.e., it is not readily incorporated opposite natural bases in the template)? Using the analogues and natural bases shown in Figure 1, we examined the effect of "mutating" specific atoms on both high-fidelity bases (adenine and guanine) and low-fidelity bases (benzimidazole, 4-methylbenzimidazole, and 4-trifluoromethylbenzimidazole). To minimize the possibility that the results of the change were base specific, we examined the effects of altering specific atoms within the context of multiple-base analogues. Importantly, each of the analogous atomic replacements gave similar results with all of the bases that were tested (see below).

Synthetic primer−template motifs of defined sequence were used to analyze the incorporation of analogue and natural dNTPs opposite the four natural bases. To minimize the possibility that the DNA sequence around the template base being copied would influence results, we measured the degree of polymerization of dNTPs across from all four natural bases in essentially the same sequence context (Figure 2). For one of the four templates (DNA_A), one additional base in the single-stranded template had to be altered to prevent insertion of two consecutive dTTPs. We determined V_{max} and K_M for incorporation of natural dNTPs opposite their natural template partners (Table 1) and analogue dNTPs, along with dATP and dGTP, opposite all four natural templates (Table 2). As expected on the basis of previously published data, pol α polymerized dATP and dGTP opposite an incorrect base several orders of magnitude slower than opposite the correct template base (*12*).

N-3 Helps Pol α Discriminate between Right and Wrong dNTPs. We first examined the effect of removing N-3 from the high-fidelity bases adenine and guanine (Table 2). During correct incorporation, removing N-3 decreases the efficiency

Table 2: Kinetic Parameters for Incorporation of Natural and Analogue dNTPs by Human Pol α[a]

dNTP	Base Structure	DNA_N	V_{MAX} (SD)	K_M (SD)	V_{MAX}/K_M	Discrimination[b]
dATP		DNA_A	0.56 (0.14)	1200 (420)	0.00047	2800
		DNA_T	10 (1.4)	5.9 (2.5)	1.7	1
		DNA_C	2.1 (0.6)	340 (150)	0.0058	1000
		DNA_G	0.060 (0.004)	210 (28)	0.00029	2800
d3DATP		DNA_A	0.29 (0.13)	720 (430)	0.00040	3200
		DNA_T	16 (3)	18 (7)	0.91	1.9
		DNA_C	2.7 (0.9)	210 (100)	0.013	460
		DNA_G	0.084 (0.016)	210 (93)	0.00040	2000
dGTP	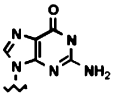	DNA_A	0.038 (0.005)	700 (140)	0.000054	24000
		DNA_T	0.75 (0.11)	620 (170)	0.0012	1400
		DNA_C	8.2 (3.1)	1.4 (0.5)	5.9	1
		DNA_G	0.47 (0.09)	650 (200)	0.00072	1100
d3DGTP	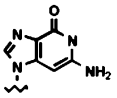	DNA_A	0.091 (0.010)	140 (37)	0.00065	2000
		DNA_T	0.17 (0.04)	190 (78)	0.00089	1900
		DNA_C	4.5 (0.3)	4.0 (0.7)	1.1	5.3
		DNA_G	2.6 (0.3)	92 (24)	0.028	28
dQTP		DNA_A	0.50 (0.16)	580 (310)	0.00086	1500
		DNA_T	0.51 (0.03)	200 (18)	0.0023	670
		DNA_C	1.2 (0.2)	74 (28)	0.016	360
		DNA_G	0.090 (0.009)	110 (27)	0.00081	980
d6MPTP		DNA_A	0.12 (0.06)	450 (350)	0.00027	5000
		DNA_T	1.3 (0.1)	7.3 (1.8)	0.18	9.7
		DNA_C	0.34 (0.04)	80 (24)	0.0043	1400
		DNA_G	0.044 (0.013)	240 (140)	0.00018	4400
d4ABTP	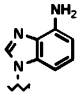	DNA_A	0.33 (0.06)	60 (25)	0.0055	240
		DNA_T	0.89 (0.03)	68 (7)	0.013	130
		DNA_C	3.4 (0.3)	26 (7)	0.13	45
		DNA_G	0.06 (0.01)	40 (16)	0.0015	530
dBTP[c]		DNA_A				130
		DNA_T				130
		DNA_C				76
		DNA_G				400
d1DPTP		DNA_A	0.30 (0.07)	300 (110)	0.0010	1300
		DNA_T	0.38 (0.06)	150 (50)	0.0025	680
		DNA_C	1.1 (0.1)	99 (23)	0.011	520
		DNA_G	0.29 (0.09)	1500 (600)	0.00019	4200
d1DATP		DNA_A	0.37 (0.07)	460 (160)	0.00080	1600
		DNA_T	1.5 (0.3)	18 (7)	0.083	20
		DNA_C	0.14 (0.01)	14 (8)	0.010	600
		DNA_G	0.046 (0.009)	270 (130)	0.00017	4700
$d4F_3BTP$[d]		DNA_A	0.35 (0.03)	130 (16)	0.0027	480
		DNA_T	0.11 (0.01)	45 (9)	0.0024	700
		DNA_C	1.2 (0.4)	97 (41)	0.012	470
		DNA_G	0.11 (0.02)	170 (54)	0.00064	1200
$d6F_3PTP$		DNA_A	0.023 (0.003)	700 (1100)	0.000030	> 25000
		DNA_T	0.048 (0.010)	22 (10)	0.0022	780
		DNA_C	0.10 (0.02)	260 (67)	0.00038	13000
		DNA_G	0.0052 (0.0010)	170 (89)	0.000031	26000
dPTP		DNA_A	0.067 (0.009)	140 (43)	0.00048	2700
		DNA_T	3.4 (0.6)	16 (6)	0.21	8.0
		DNA_C	0.40 (0.04)	67 (23)	0.0060	1000
		DNA_G	0.025 (0.004)	85 (37)	0.00029	2700
dZTP		DNA_A	0.65 (0.06)	33 (10)	0.020	66
		DNA_T	0.54 (0.04)	18 (1)	0.030	57
		DNA_C	1.8 (0.2)	12 (7)	0.15	40
		DNA_G	0.42 (0.07)	83 (19)	0.0051	160
d3DPTP		DNA_A	0.015 (0.001)	80 (17)	0.00019	6800
		DNA_T	0.78 (0.17)	9.2 (5.1)	0.085	20
		DNA_C	0.087 (0.008)	31 (11)	0.0028	2100
		DNA_G	0.010 (0.002)	49 (21)	0.00020	3800

[a] Polymerization assays were performed and analyzed as described in Experimental Procedures. The units for V_{max} and K_M are % of primer elongated min^{-1} and μM^{-1}, respectively. The units for V_{max}/K_M are % elongated μM^{-1} min^{-1}. [b] Discrimination reflects how much more efficiently the correct dNTP is incorporated compared to the analogue or incorrect dNTP (for example, dGTP incorporates at a rate 24 000 times slower opposite template A than does dTTP). Also note that the discrimination number of a natural dNTP opposite its correct template partner is designated as 1. [c] Kinetic parameters determined previously (*12*). [d] Kinetic parameters determined previously (*11*).

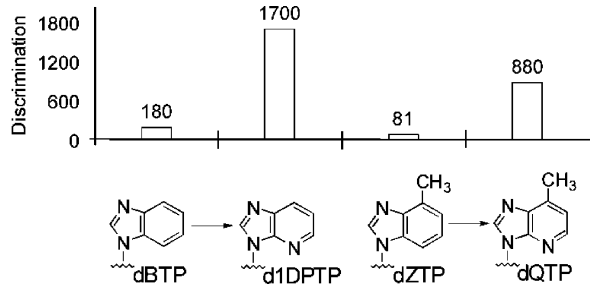

FIGURE 3: Effect of adding N-3 to the low-fidelity bases benzimidazole (dBTP) and 4-methylbenzimidazole (dZTP) to generate 1-deazapurine (d1DPTP) and 1-deaza-6-methylpurine (dQTP), respectively. The white bars in the graph are the average value by which pol α discriminates against polymerization of each analogue opposite A, C, T, and G relative to polymerization of a correct dNTP.

of incorporation by 2-fold for 3-deazaadenine and 5-fold for 3-deazaguanine. As compared to misincorporation of dATP and dGTP, removing N-3 decreases fidelity opposite some bases but has relatively little effect opposite others. However, if one compares the efficiency with which pol α correctly incorporates 3-deaza-dATP and 3-deaza-dGTP with the rates at which it incorrectly incorporates these dNTPs, removing N-3 significantly reduces the fidelity across the board due to the lower efficiency of correct incorporation of the 3-deaza-dNTPs compared to the natural dNTPs.

Because removing N-3 from high-fidelity bases decreases fidelity, we tested the hypothesis that adding N-3 back to low-fidelity bases would increase fidelity (Figure 3 and Table 2). Pol α discriminates relatively poorly against polymerization of benzimidazole-dNTP and 4-methylbenzimidazole-dNTP opposite all four natural bases. (Discrimination is defined as V_{max}/K_M for polymerization of the correct, natural dNTP divided by V_{max}/K_m for polymerization of an analogue or incorrect, natural dNTP.) Upon addition of the equivalent of a purine N-3, however, pol α now discriminates against polymerization of the resulting 1-deazapurine-dNTP and 1-deaza-6-methylpurine-dNTP much more efficiently. Thus, for both high- and low-fidelity bases, N-3 appears to be important for maintaining fidelity.

N-1 Also Helps Pol α Discriminate between Right and Wrong dNTPs. Adding N-1 to 1-deazadATP (d1DATP), thereby generating dATP, increases the level of incorporation opposite T by 20-fold (Figure 4 and Table 2) but has relatively weak effects on the incorporation opposite A, C, and G as compared to dATP. In contrast, adding N-1 back to three bases with fidelity lower than normal (benzimidazole, 1-deazapurine, and 1-deaza-6-methylpurine, to generate 3-deazapurine, purine, and 6-methylpurine, respectively) significantly enhances the ability of pol α to identify dNTPs containing the resulting analogues as being wrong for polymerization opposite either A, C, or G. Concomitantly, adding N-1 back greatly enhanced polymerization opposite T. In each of these three bases that contained N-1, 3-deazapurine, purine, and 6-methylpurine, the hybridization state of N-1 will allow formation of a Watson−Crick hydrogen bond with the HN-3 group of T.

The roles of N-1 and N-3 were also examined by comparing 4-trifluoromethylbenzimidazole-dNTP with 6-trifluoromethylpurine-dNTP (Figure 5 and Table 2). Consistent with the results described above, adding these groups back

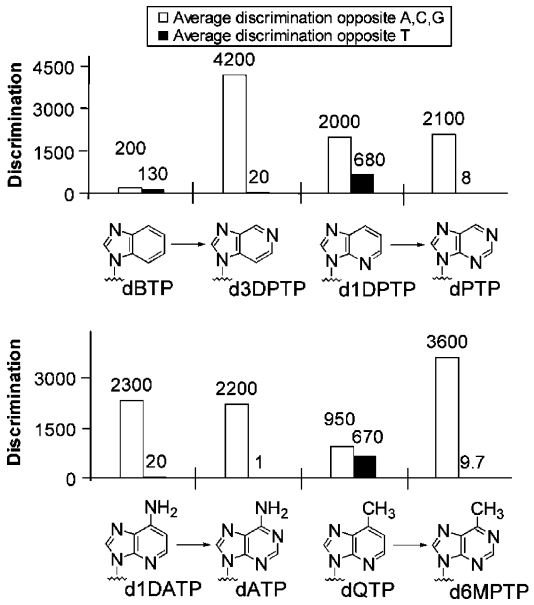

FIGURE 4: Adding N-1 to benzimidazole (dBTP) or 1-deaza-6-methylpurine (dQTP) increases the degree of polymerization opposite T and decreases the degree of polymerization opposite A, C, and G. The white bars in the graph are the average value by which pol α discriminates against polymerization of each analogue opposite A, C, and G relative to polymerization of a correct dNTP, while the black bars show how much slower pol α polymerizes each analogue opposite T as compared to dATP.

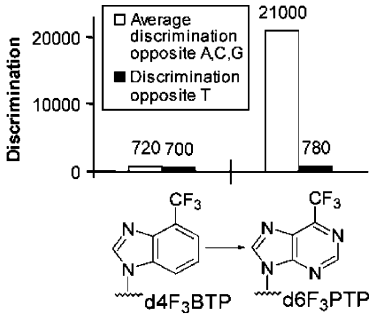

FIGURE 5: Generating $d6F_3PTP$ by adding N-1 and N-3 to $d4F_3$-BTP decreases the degree of polymerization opposite A, C, and G while maintaining polymerization opposite T. The white bars in the graph are the average value by which pol α discriminates against polymerization of each analogue opposite A, C, and G relative to polymerization of a correct dNTP, while the black bars show how much slower pol α polymerizes each analogue opposite T as compared to dATP.

greatly enhanced the ability of pol α to discriminate against polymerization of 6-trifluoromethylpurine-dNTP opposite A, C, and G. Indeed, pol α discriminates against polymerization of 6-trifluoromethylpurine-dNTP much more strongly than natural dNTPs. Comparatively, pol α polymerized 6-trifluoromethylpurine-dNTP opposite T relatively efficiently.

The Exocyclic Amino Group at C-6 Primarily Enhances Polymerization Opposite T. As is the case for N-1, the exocyclic amino group at C-6 (N-6) can form a hydrogen bond with T. The level of incorporation opposite T increases 10−20-fold upon addition of N-6 to 3-deazapurines (Figure 6 and Table 2), and this rate increases 35-fold when it is added to 1-deazapurine and 1-deaza-6-methylpurine. However, unlike N-1, adding N-6 does not significantly influence incorporation rates opposite template A, C, or G. When the discrimination numbers obtained opposite these three templates are averaged, adding N-6 to 1-deaza-6-methylpurine

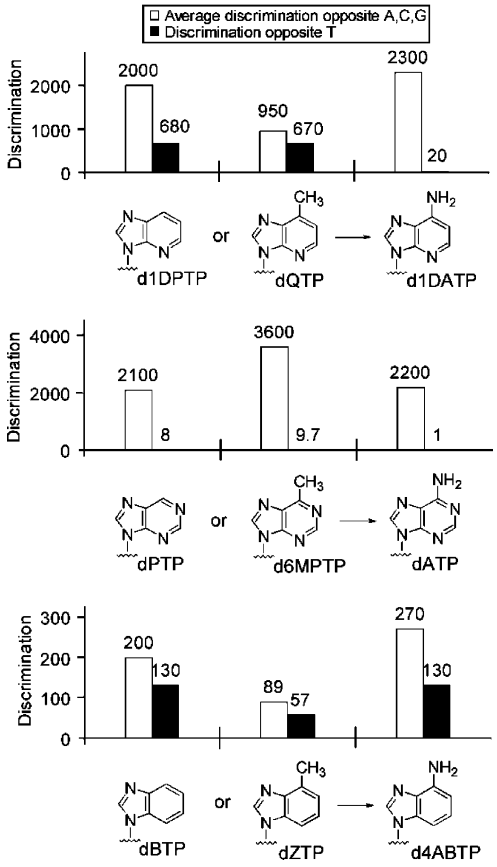

FIGURE 6: Effect of adding the equivalent of adenine's exocyclic amine at C-6 (N-6). The white bars in the graph are the average value by which pol α discriminates against polymerization of each analogue opposite A, C, and G relative to polymerization of a correct dNTP, while the black bars show how much slower pol α polymerizes each analogue opposite T as compared to dATP.

and to 4-methylbenzimidazole (generating 1-deazaadenine and 4-aminobenzimidazole, respectively) only increases the level of discrimination by 2−3-fold. However, in all other cases when N-6 is added (i.e., converting 1-deazapurine, 3-deazapurine, and benzimidazole to 1-deazaadenine, 3-deazaadenine, and 4-aminobenzimidazole, respectively), the level of discrimination does not significantly increase and even decreases slightly in the case of 3-deazaadenine versus 3-deazapurine (Table 2). Overall, the average level of discrimination against polymerization opposite A, C, and G rarely increases more than 2-fold and decreases by no more than 3-fold (in a single case) upon addition of N-6. In contrast, adding N-1 or N-3 consistently and often times dramatically increases the level of discrimination, frequently by ≥10-fold (Table 2 and Figures 3 and 4). Thus, N-6 most likely has one primary role, helping pol α positively identify a dNTP for polymerization opposite its correct base partner (as opposed to helping pol α identify the incoming dNTP as being wrong).

Requirements for Efficient Polymerization of the Next Correct dNTP onto Adenine Analogues. We generated a series of primer templates in which the 3′-terminal nucleotide on the primer contained either adenine or an adenine analogue and measured the rate of polymerization of dTTP, the next correct dNTP (Table 3). Removing a single Watson−Crick hydrogen bonding group reduces the efficiency of dTTP polymerization, while removal of both N-1 and N-6 severely impaired dTTP incorporation. The loss of N-3 also inhibited dTTP polymerization, but to a lesser extent than the loss of either N-1 or N-6.

Requirements for Efficient Polymerization of the Second Correct dNTP onto Adenine Analogues. We used the running-start methodology pioneered by Goodman and coworkers to assess polymerization of the second correct dNTP onto primer−template motifs (Table 4). Assays contained a primer−template motif whose 3′-terminal nucleotide was either adenine or an adenine analogue, dTTP, and varying concentrations of dATP. Under these conditions, pol α can polymerize up to two nucleotides onto the primer terminus. Having a base at the primer terminus that could only form one Watson−Crick hydrogen bond with the template T (i.e., purine, 6-methylpurine, and 1-deazaadenine) resulted in only small effects on polymerization of the second correct dNTP. However, the absence of N-3 at the primer terminus (either 3-deazaadenine or 3-deazapurine) greatly impaired polymerization of the second correct dNTP.

In those cases where pol α could efficiently add the second correct dNTP, we qualitatively examined further polymerization by also including dGTP in the assays to potentially allow polymerization to the end of the template. Figure 7 shows that the absence of one of the Watson−Crick hydrogen bonds at the primer terminus did not significantly impede polymerization of the third or latter dNTPs, although there are some differences. Most notably, the strong pause site observed at the primer +9 position observed with either adenine, purine, or 1-deazaadenine at the primer terminus is not observed with 6-methylpurine at the primer terminus.

Hydrophobicity Does Not Correlate with Fidelity. We calculated the hydrophobicity parameter, logP, of each of the bases of Figure 1 (except 3-deazaadenine, 3-deazaguanine, and guanine) and compared these values with the ability of pol α to identify corresponding dNTPs as being wrong. Since many of the analogues can form a Watson−Crick hydrogen bond(s) with T and, therefore, can be considered as dATP analogues, we defined wrong as polymerization opposite A, C, and G. Figure 8 shows that the ability of pol α to discriminate against polymerization of the analogues does not closely correlate with hydrophobicity, consistent with the results of previous studies (*11*). While the more hydrophobic bases tend to give lower-fidelity dNTPs, there are multiple exceptions to this trend.

DISCUSSION

Using a series of dNTP analogues, we have identified the features of an incoming purine dNTP that pol α uses to identify it as either right or wrong. Pol α uses both N-1 and N-3 to prevent misincorporation, while it uses N-1 and the exocyclic amine at C-6 (N-6) to enhance correct incorporation opposite T. After incorporation of a nucleotide, however, the correct geometry of the base pair at the primer 3′-terminus appears to be critical for rapid polymerization of additional dNTPs.

Two sets of data demonstrated the importance of N-3 for fidelity: removing it from the high-fidelity bases adenine and guanine reduced fidelity, and adding N-3 back to the low-fidelity bases benzimidazole, 4-methylbenzimidazole, and 4-trifluoromethylbenzimidazole (although, in the latter case N-1 was simultaneously added back) significantly enhanced the ability of the polymerase to identify the

Table 3: Next Correct dNTP Insertion by Human Pol α (dTTP insertion following analogue X)[a]

X in 5′-primer-X-3′	V_{max} (SD)	K_M (SD)	V_{max}/K_M	discrimination[b]
adenine	16 (2)	3.2 (1.6)	5.0	1
purine	8.4 (1.2)	50 (16)	0.17	29
6-methylpurine	1.7 (0.1)	9.6 (3.8)	0.18	28
1-deazaadenine	3.8 (1.6)	35 (10)	0.11	45
3-deazaadenine	22 (7)	39 (23)	0.55	9.1
3-deazapurine	12 (2)	130 (42)	0.09	56
4-aminobenzimidazole	0.09 (0.09)	1100 (1600)	0.000081	62000
1-deazapurine	0.54 (0.78)	2200 (4100)	0.00025	20000

[a] Polymerization read-through assays were performed as described in Experimental Procedures. Kinetic parameters for dTTP polymerization were determined when either A or the noted analogue was present at the primer terminus. [b] Discrimination is V_{max}/K_M for dTTP polymerization when A is at the primer terminus divided by V_{max}/K_M when an analogue (X) is at the primer terminus. The units for V_{max}/K_M are % elongated μM^{-1} min^{-1}.

Table 4: Insertion of the Second Correct dNTP by Human Pol α (dATP insertion after T)[a]

X in 5′-primer-X-T-3′	V_{max} (SD)	K_M (SD)	V_{max}/K_M	discrimination[b]
adenine	30 (3)	4.5 (2.2)	6.7	1
purine	16 (2)	6.1 (2.7)	2.6	3
6-methylpurine	6.6 (0.6)	5.9 (1.5)	1.1	6
1-deazaadenine	13 (2)	10 (4)	1.3	5
3-deazaadenine	0.17 (0.16)	3.4 (1.7)	0.050	130
3-deazapurine	0.21 (0.02)	4.3 (1.7)	0.049	140

[a] Polymerization read-through assays were performed as described in Experimental Procedures. Kinetic parameters for dATP polymerization opposite a template T were determined when either A or the noted analogue was present one nucleotide before the primer terminus. [b] Discrimination is V_{max}/K_M for dATP polymerization when X is adenine divided by V_{max}/K_M for dATP polymerization when X is an analogue. The units for V_{max}/K_M are % elongated μM^{-1} min^{-1}.

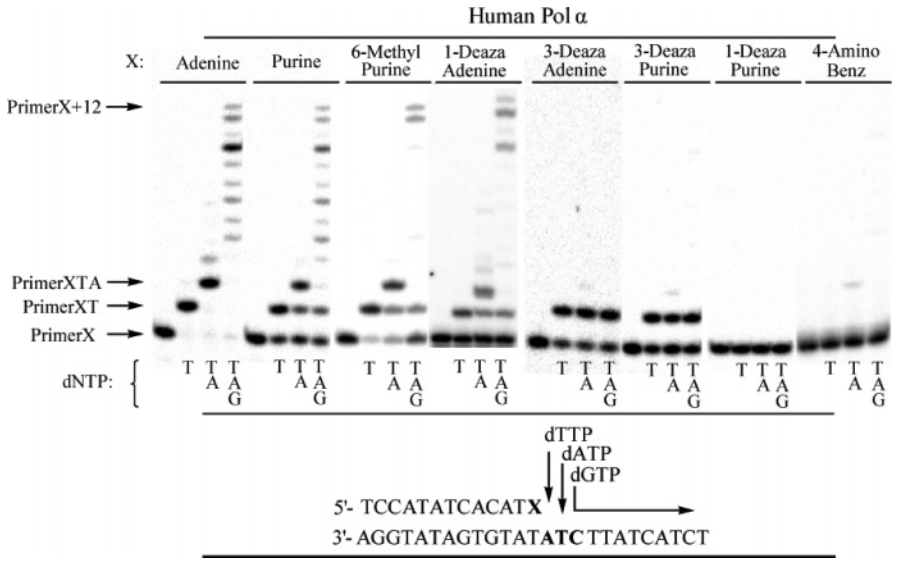

FIGURE 7: Read-through comparison of the analogues by human pol α. Assays contained 1 nM primerX−template (where X represents the analogue at the primer 3′-terminus), 0.5 nM pol α, and the noted dNTPs at 25 μM.

resulting analogues as being wrong. These data indicate that N-3 contributes a factor of around 5−20 to the fidelity of pol α.[2]

A key question is how pol α uses N-3 to identify an incoming purine dNTP as being wrong. Since N-3 enhances the ability of pol α to identify as wrong bases that cannot form Watson−Crick hydrogen bonds (for example, benzimidazole and 4-methylbenzimidazole), the effects of N-3 cannot be due to electronic effects on Watson−Crick hydrogen bonding groups. Alternatively, pol α may directly interact with N-3. At present, no high-resolution structures of the active site of pol α exist, although the structures of two other family-B polymerases, RB69 and herpes DNA polymerase, have been determined (*32*, *33*). Importantly, the active site region of pol α, RB69 and herpes DNA polymerases that interact with the incipient base pair between the incoming dNTP and template base exhibit remarkable homology, suggesting that they will have very similar structures (Table 5; *34*). While only the apoenzyme form of herpes DNA polymerase has been determined, the structure of both the apoenzyme and E−DNA−dNTP forms of RB69

[2] The amount of fidelity lost or gained by removing or adding N-3, respectively, depends on how one looks at the data. Comparing the misincorporation rates versus the correct polymerization rates of 3-deazadATP and 3-deazadGTP reveals a larger loss of fidelity upon removal of N-3 than comparing misincorporation rates of 3-deazadATP and 3-deazadGTP versus the correct polymerization rates of dATP and dGTP. This results from the slower correct polymerization of the 3-deaza-dNTPs.

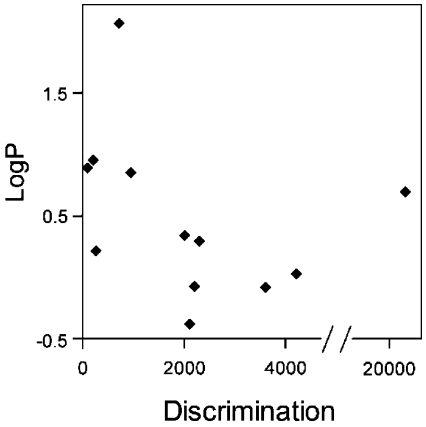

FIGURE 8: Plot of base hydrophobicity (logP) vs fidelity of base-dNTP opposite templates A, C, and G (the average of the three discrimination numbers, taken from Table 2).

Table 5: Sequence Alignment of Several Family-B Polymerases[a]

RB69	553	MTAQINRKLLINSLYGALG
T4	549	NTNQLNRKILINSLYGALG
HSV1	804	DKQQAAIKVVCNSVYGFTG
Vent	503	DYRQRAIKLLANSYYGYMG
Pol α (human)	943	DIRQKALKLTANSMYGCLG
Pol I (yeast)	937	DIRQQALKLTANSMYGCLG

[a] The sequence shown represents a large portion of the active site that surrounds the dNTP and template base being replicated, defined as a portion of region III (*34*).

polymerase has been determined (*32*, *35*). In the ternary complex, dTTP forms a correct base pair with a template adenine and is presumably poised for incorporation. Interestingly, O-2 of the thymine sits just above the edge of Y567 (the equivalent of Y957 in pol α). Since N-3 of a purine and O-2 of a pyrimidine share similar locations in a correct base pair, N-3 will presumably also be located just above this tyrosine (Figure 9). Significantly, the edge of tyrosine is electron deficient, and O-2 of a pyrimidine and N-3 of a purine are both electron rich, allowing for a very favorable interaction (*36*). Thus, we suspect that interactions between N-3 and this tyrosine serve to enhance the fidelity of pol α. Indeed, mutational studies of this tyrosine in RB69 polymerase also support an interaction between these groups (*37*). Converting Y567 to alanine in RB69 polymerase had only weak effects on polymerization of a correct dNTP (5-fold, V_{max}/K_M) but decreased fidelity from none to 180-fold depending upon the mismatch. Strikingly, these results are qualitatively identical to the effects of converting N-3 of a purine dNTP into a C−H group (small effect on correct dNTP polymerization, often large and mismatch-dependent decreases in fidelity).

Pol α uses N-1 both to discriminate against wrong dNTPs and to enhance polymerization opposite T. Adding the equivalent of N-1 to either benzimidazole, 4-aminobenzimidazole, or 1-deaza-6-methylpurine significantly enhanced the ability of pol α to identify the resulting dNTPs as wrong opposite A, C, and G. The presence of N-1 also greatly increased the efficiency with which pol α polymerized the various analogues opposite T. Presumably, this reflects the formation of a Watson−Crick hydrogen bond between the purine N-1 and HN-3 group of thymine. In each of the analogues that were tested, N-1 will act as a hydrogen bond acceptor.

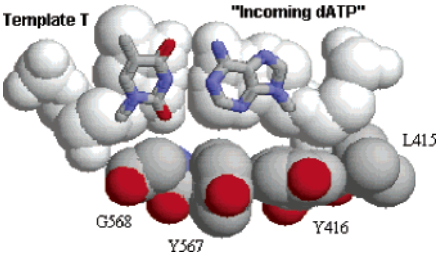

FIGURE 9: Representation of an incoming dATP and a template T inside the active site of RB69 (adapted from the data in PDB entry 1IG9). We replaced the dTTP·A base pair with a dATP·T base pair while maintaining the location of the sugar phosphates of each nucleotide. Only selected residues are shown for simplicity.

The effects of N-1 and N-3 on discrimination against wrong dNTPs do not appear to be additive. Adding either N-1 or N-3 to benzimidazole and generating 1-deazapurine- and 3-deazapurine-dNTP, respectively, similarly decreased the degree of polymerization opposite A, C, and G. Simultaneously adding back both N-1 and N-3 to benzimidazole to generate purine-dNTP resulted in a level of discrimination much lower than one would predict if these effects were additive. Similar less-than-additive effects are observed for adding N-1 and N-3 back to 4-aminobenzimidazole. Analogously, removing N-3 from adenine had smaller effects on fidelity when compared to the changes observed upon adding N-3 to the benzimidazole derivatives. Thus, pol α can use either N-1 or N-3 to prevent misincorporation, and the functional redundancy may serve to simply ensure high fidelity.

Unlike N-1 and N-3 that help pol α identify an incoming dNTP as being wrong, N-6 appears to primarily serve to identify the incoming dNTP as being right opposite T. Adding N-6 to either purine or 1-deazapurine did not enhance pol α's ability to identify the resulting dATP or 1-deaza-dATP as being wrong opposite A, C, and G but significantly enhanced polymerization opposite T. Similarly, adding the equivalent of N-6 to benzimidazole, thereby generating 4-aminobenzimidazole-dNTP, did not enhance pol α's ability to identify the resulting base as being wrong. Somewhat surprisingly, pol α did not preferentially incorporate this dNTP opposite T. This case is slightly more complicated, however, because the absence of both N-1 and N-3 has a large effect on the chemical properties of N-6. Adenine's N-6 is a hydrogen bond donor. However, in aqueous solution, removing N-1 and N-3 from adenine (generating 4-aminobenzimidazole) changes the pK_a of the N-6 group to approximately 4.4, effectively turning this group into a hydrogen bond acceptor at physiological pH (J. Beckman and R. Kuchta, unpublished data).

Together, these data indicate that pol α uses a combination of positive and negative selectivity to accurately incorporate purine dNTPs. The presence of N-1 and/or N-3 allows pol α to identify an incoming dNTP as being wrong, while N-1 and N-6 (of adenine) allow pol α to identify the incoming dNTP as being right opposite T. As described in greater detail below, pol α specifically does not use the shape of the incipient base pair to identify it as being right. Importantly, this model can accommodate all published data on the fidelity of pol α and other family-B polymerases with natural and synthetic dNTPs. The relatively rapid and unselective polymerization of dNTPs containing bases that neither resemble

Table 6: Comparison of the Efficiency of Analogue Polymerization Revealing a Lack of Correlation between Incoming Base Shape and Didelity[a]

N in dNTP	N-3	N-1	N-6	adenine shape[a]	$(V_{max}/K_M)_T$[b]/ $(V_{max}/K_M)_C$
A	+	+	+	+	290
3DA		+	+	+	70
6MP	+	+		+	42
P	+	+			41
3DP		+			35
1DA	+		+	+	8.3
$6F_3P$	+	+		+	5.8
1DP	+				0.23
Z				+	0.20
$4F_3B$				+	0.20
Q	+			+	0.14
4AB			+	+	0.10

[a] A base is not the adenine shape if it does not contain a group at N-6 similar in size to adenine's exocyclic amine. [b] V_{max}/K_M values are taken from Table 2. $(V_{max}/K_M)_T$ is the polymerization of the dNTP opposite T, and $(V_{max}/K_M)_C$ is the polymerization of the dNTP opposite C.

the shape of a correct base nor form Watson−Crick hydrogen bonds [for example, 5-nitrobenzimidazole, 5-methoxybenzimidazole, and 5,6-dinitrobenzimidazole (*11*, *12*)] opposite both canonical and unnatural template bases results from their lack of the chemical features needed for pol α to identify them as being wrong. Similarly, the high fidelity of natural dNTPs opposite both canonical and unnatural template bases [5- and 6-nitrobenzimidazole (*12*)] results from these bases containing negative selectors preventing misincorporation and the positive selectors specifying the template base opposite which the incoming dNTP should be polymerized.

Importantly, shape is not directly used by pol α as either a negative or a positive selector. Pol α readily misincorporates dNTPs whose bases are similar in shape to adenine (for example, benzimidazole, 4-methylbenzimidazole, 4-trifluoromethylbenzimidazole, and 4-aminobenzimidazole) as well as dNTPs whose base shapes are very different from that of adenine (for example, 5,6-dinitrobenzimidazole). Changes that will have minimal effects on shape, replacing two carbons with nitrogen, greatly improve fidelity. The negligible importance of shape is shown explicitly in Table 6. Since, with the exception of dGTP and d3DGTP, all of the dNTPs that were tested can be viewed as dATP analogues, we have compared the efficiency of polymerization opposite either C or T, the potential shape complements of purines. Whereas how closely the base resembles adenine does not predict the efficiency of polymerization opposite T versus C, N-1, N-3, and N-6 do predict whether pol α will recognize the dNTP analogue as dATP. Thus, pol α presumably uses specific chemical properties of these nitrogens to identify a base as being wrong.

Mechanistically, how might pol α use these positive and negative selectors to identify an incoming dNTP as being wrong or right? The relatively nonspecific incorporation of dNTPs lacking N-1 and N-3 indicates that after these dNTPs bind, the enzyme can readily adopt a catalytically active conformation, even though the bases of the template and incoming dNTP cannot form a correctly shaped base pair [for example, the relatively rapid polymerization of 5,6-dinitrobenzimidazole, 5-nitroindole, or 4-methylbenzimidazole opposite A and G (refs *11* and *12* and Table 2, respectively)]. Upon addition of either N-1 or N-3 back to the unnatural base, pol α adopts a catalytically active conformation much less readily. Potentially, this could occur if the free electron pair of the nitrogen either blocked a needed conformational change or prevented the unnatural base from finding an unobtrusive pocket that allowed catalysis. The positive selectors, N-1 and N-6 of adenine, would then serve to overcome the effects of the negative selectors when the appropriate template base, thymine, is present. For example, by enhancing the formation of a Watson−Crick base pair, the positive selectors would remove the negative selectors from positions that block polymerization (i.e., when opposite a wrong template base) and into a position that allows formation of a catalytically active enzyme. This effect can also be viewed as an indirect readout of base pair shape. Formation of a correctly shaped base pair will necessarily remove N-1 and N-3 from any location that can inhibit dNTP polymerization, while formation of an incorrectly shaped base pair will leave N-1 and N-3 in positions that inhibit polymerization.

In contrast to the lack of shape selectivity during the dNTP polymerization reaction, shape appears to be critical for addition of the next correct dNTP. Previous work showed that polymerases closely related to human pol α, *Drosophila* and calf thymus pol α, polymerize the next correct dNTP onto mismatches 10^3-10^5-fold more slowly than onto a correct base pair (*38*, *39*). Analogously, after incorporating an unnatural base lacking the ability to form Watson−Crick hydrogen bonds [for example, 5-methoxybenzimidazole and 5,6-dinitrobenzimidazole (*11*) or 1-deazapurine and 4-aminobenzimidazole (Table 2)], pol α polymerizes the next correct dNTP at similar slow rates. However, when groups that can form Watson−Crick hydrogen bond(s) with the template base are added back [for example, analogues with either N-1, both N-3 and N-6, or both N-1 and N-6 (Table 3 and Figure 7)], the rate of addition of the next correct dNTP increases dramatically. Presumably, adding back a Watson−Crick hydrogen bond will increase the degree of similarity between the analogue-T base pair and a natural, correct base pair, thereby optimizing the position of the 3′-OH for rapid polymerization of the next dNTP. As one would predict if pol α is recognizing the shape of the base pair at the primer terminus, generating a base pair that contains two Watson−Crick hydrogen bonds enhances polymerization more than a base pair capable of a single bond. Potentially, the slightly slower elongation of the primer containing 3-deazaadenine rather than adenine could reflect either an interaction between pol α and N-3 or the effect of removing N-3 on the chemical properties of N-1 and/or N-6.

A key feature of the fidelity strategy employed by pol α is using two orthogonal screens. As noted earlier, the fidelity of a polymerase results from both usually choosing the right (d)NTP and only slowly elongating the product of wrong incorporation, thereby allowing proofreading. During incorporation, pol α employs a combination of positive and negative selectivity, while for elongation of the newly added nucleotide, pol α uses shape selectivity. A consequence of this strategy is that modified bases that can bypass the first screen are more likely to be detected by the second screen since this latter screen examines a different set of parameters than the first screen. If both screens were based on the same parameter(s), a wrong base that easily bypasses the first

screen would just as easily bypass the second screen. While pol α itself lacks 3′−5′ exonuclease activity and hence cannot directly proofread, the very slow elongation of misshaped base pairs presumably allows pol α to dissociate from the DNA and another exonuclease to excise the nucleotide at the primer 3′-terminus.

Efficient incorporation of the second dNTP onto a primer by pol α clearly requires that an adenine base at the primer terminus contain N-3. Similarly, we found that pol α does not efficiently add the second dNTP if 3-deazaguanine is present at the primer terminus (J. Beckman and R. Kuchta, unpublished data). Recently, Benner and co-workers demonstrated that two other family-B polymerases, Pfu polymerase and "GB-D" (deep vent polymerase), also require N-3 for incorporation of the second dNTP (*47*). This discrimination most likely results from a requirement for a hydrogen bond between N-3 and a conserved lysine residue. The structure of the RB69 polymerase−DNA complex shows that this hydrogen bond is formed by K706, pol α's equivalent of K1052 (*35*, *47*). The absence of this hydrogen bond presumably prevents pol α from adopting a catalytically active conformation. However, N-3 is not a universal requirement for family-B polymerases, since "Tli" (vent polymerase) does not require N-3 (*47*).

The extent to which other polymerase families employ strategies similar to that of pol α is at present unclear. Human and herpes primase appear to require the formation of Watson−Crick hydrogen bonds to polymerize a NTP (*6*, *7*). Indeed, these enzymes misincorporate the natural NTPs orders of magnitude faster than they will incorporate NTPs containing unnatural bases incapable of Watson−Crick hydrogen bonding with the template, a situation diametrically opposed to that for pol α. Klenow fragment, a family-A polymerase, has been suggested to use shape as the primary determinant for fidelity (*8*−*10*, *40*−*42*). However, various groups have also shown that KF will also efficiently incorporate bases whose shape does not resemble a canonical base (*11*, *12*, *43*−*46*).

Together, the data presented here indicate that pol α achieves fidelity during the polymerization of purine dNTPs using a pair of cleverly designed orthogonal screens. While we have restricted our discussion to purine dNTPs, unpublished studies indicate that pol α uses similar strategies during polymerization of pyrimidine dNTPs (M. Loi, G. Timblin, and R. Kuchta, unpublished data). Ultimately, a detailed understanding of the requirements for accurate and efficient polymerization of both purine and pyrimidine dNTPs by pol α should allow the generation of novel base pairs that pol α replicates with high efficiency and fidelity.

REFERENCES

1. Roberts, J. D., and Kunkel, T. A. (1996) *DNA Replication in Eukaryotic Cells: Concepts, Enzymes and Systems* (Depamphilis, M., Ed.) pp 217−247, Cold Spring Harbor Laboratory Press, Plainview, NY.
2. Drake, J. W. (1991) A constant rate of spontaneous mutation in DNA-based microbes, *Proc. Natl. Acad. Sci. U.S.A. 88*, 7160−7164
3. Kunkel, T. A., and Bebenek, K. (1988) Recent studies of the fidelity of DNA synthesis, *Biochim. Biophys. Acta 951*, 1−15.
4. Watson, J. D., and Crick, F. H. C. (1953) Molecular Structure of Nucleoic Acids, *Nature 171*, 737−738.
5. Watson, J. D., and Crick, F. H. C. (1953) Genetical Implications of the Structure of Deoxyribonucleic Acid, *Nature 171*, 964−967.
6. Moore, C. L., Zivkovic, A., Engels, J. W., and Kuchta, R. D. (2004) Human DNA primase uses Watson-Crick hydrogen bonds to distinguish between correct and incorrect nucleoside triphosphates, *Biochemistry 43*, 12367−12374.
7. Ramirez-Aguilar, K. A., Moore, C. L., and Kuchta, R. D. (2005) Herpes simplex virus 1 primase employs Watson-Crick hydrogen bonding to identify cognate nucleoside triphosphates, *Biochemistry 44*, 15585−15593.
8. Moran, S., Ren, R. X., and Kool, E. T. (1997) A thymidine triphosphate shape analog lacking Watson-Crick pairing ability is replicated with high sequence selectivity, *Proc. Natl. Acad. Sci. U.S.A. 94*, 10506−10511.
9. Morales, J. C., and Kool, E. T. (1998) Efficient replication between non-hydrogen-bonded nucleoside shape analogs, *Nat. Struct. Biol. 5*, 950−954.
10. Morales, J. C., and Kool, E. T. (2000) Varied Molecular Interactions at the Active Sites of Several DNA Polymerases: Nonpolar Nucleoside Isosteres as Probes, *J. Am. Chem. Soc. 122*, 1001−1007.
11. Kincaid, K., Beckman, J., Zivkovic, A., Halcomb, R. L., Engels, J. W., and Kuchta, R. D. (2005) Exploration of factors driving incorporation of unnatural dNTPS into DNA by Klenow fragment (DNA polymerase I) and DNA polymerase α, *Nucleic Acids Res. 33*, 2620−2628.
12. Chiaramonte, M., Moore, C. L., Kincaid, K., and Kuchta, R. D. (2003) Facile polymerization of dNTPs bearing unnatural base analogues by DNA polymerase α and Klenow fragment (DNA polymerase I), *Biochemistry 42*, 10472−10481.
13. Zerbe, L. K., Goodman, M. F., Efrati, E., and Kuchta, R. D. (1999) Abasic template lesions are strong chain terminators for DNA primase but not for DNA polymerase α during the synthesis of new DNA strands, *Biochemistry 38*, 12908−12914.
14. Wenzel, T., and Seela, F. (1996) Synthesis of 6-substituted 1-deazapurine 2′-deoxyribonucleosides, *Helv. Chim. Acta 79*, 169−178.
15. Seela, F., Rosemeyer, H., and Fischer, S. (1990) Synthesis of 3-Deaza-2-deoxyadenosine and 3-Deaza-2,3-dideoxyadenosine: Glycosylation of the 4-Chloroimidazo[4,5-c]pyridinyl Anion, *Helv. Chim. Acta 73*, 1602−1611.
16. Morales, J. C., and Kool, E. T. (1999) Minor Groove Interactions between Polymerase and DNA: More Essential to Replication than Watson-Crick Hydrogen Bonds? *J. Am. Chem. Soc. 121*, 2323−2324.
17. Cosstick, R., Li, X., Tuli, D. K., Williams, D. M., Connolly, B. A., and Newman, P. C. (1990) Molecular recognition in the minor groove of the DNA helix. Studies on the synthesis of oligonucleotides and polynucleotides containing 3-deaza-2′-deoxyadenosine. Interaction of the oligonucleotides with the restriction endonuclease EcoRV, *Nucleic Acids Res. 18*, 4771−4778.
18. Washington, M. T., Wolfe, W. T., Spratt, T. E., Prakash, L., and Prakash, S. (2003) Yeast DNA polymerase *η* makes functional contacts with the DNA minor groove only at the incoming nucleoside triphosphates, *Proc. Natl. Acad. Sci. U.S.A. 100*, 5113−5118.
19. Ludwig, J. (1981) A new route to nucleoside 5′-triphosphates, *Acta Biochim. Biophys. Acad. Sci. Hung. 16*, 131−133.
20. Kazimierczuk, Z., Cottam, H. B., Revankar, G. R., and Robins, R. K. (1984) Synthesis of 2′-deoxytubercidin, 2′-deoxyadenosine, and related 2′-deoxynucleosides via a novel direct stereospecific sodium salt glycosylation procedure, *J. Am. Chem. Soc. 106*, 6379−6382.
21. Antonini, I., Cristalli, G., Franchetti, P., Grifantini, M., Martelli, S., and Petrelli, F. (1984) Deaza analogues of adenosine as inhibitors of blood platelet aggregation, *J. Pharm. Sci. 73*, 366−369.
22. Middleton, R. W., and Wibberley, D. G. (1980) Synthesis of Imnidazo[4,5-b]- and [4,5-c]pyridines, *J. Heterocycl. Chem. 17*, 1757−1760.
23. Hocková, D., Hocek, M., Dvořáková, H., and Votruba, I. (1999) Synthesis and cytostatic activity of nucleosides and acyclic nucleoside analogues derived from 6-(trifluoromethyl)purines, *Tetrahedron 55*, 11109−11118.
24. Hocek, M., and Dvořáková, H. (2003) An Efficient Synthesis of 2-Substituted 6-Methylpurine Bases and Nucleosides by Fe- or Pd-Catalyzed Cross-Coupling Reactions of 2,6-Dichloropurines, *J. Org. Chem. 68*, 5773−5776.
25. Votruba, I., Holý, A., Dvořáková, H., Günter, J., Hocková, D., Hřebabecký, H., Cihlář, T., and Msojídková, M. (1994) Synthesis

of 2-Deoxy-β-D-ribonucleosides and 2,3-Dideoxy-β-D-pentofuranosides on Immobilized Bacterial Cells, *Collect. Czech. Chem. Commun. 59*, 2303−2330.
26. Hassan, A. E. A., Abou-Elkair, R. A. I., Montgomery, J. A., and Secrist, J. A., III (2000) Convenient syntheses of 6-methylpurine and related nucleosides, *Nucleosides, Nucleotides Nucleic Acids 19*, 1123−1134.
27. Hocek, M., and Holý, A. (1999) Perfluoroalkylation of 6-Iodopurines by Trimethyl(perfluoroalkyl)silanes. Synthesis of 6-(Perfluoroalkyl)purine Bases, Nucleosides and Acyclic Nucleotide Analogues Collect, *Czech. Chem. Commun. 64*, 229−241.
28. Maniatis, T., Fritsch, E. F., and Sambrook, J. (1982) *Molecular Cloning: A Laboratory Manual*, Cold Spring Harbor Laboratory Press, Plainview, NY.
29. Kuchta, R. D., Mizrahi, V., Benkovic, P. A., Johnson, K. A., and Benkovic, S. J. (1987) Kinetic mechanism of DNA polymerase I (Klenow), *Biochemistry 26*, 8410−8417.
30. Goodman, M. F., Creighton, S., Bloom, L. B., and Petruska, J. (1993) Biochemical basis of DNA replication fidelity, *Crit. Rev. Biochem. Mol. Biol. 28*, 83−126.
31. Leo, A. J. (1991) Hydrophobic parameter: Measurement and calculation, *Methods Enzymol. 202*, 544−591.
32. Franklin, M. C., Wang, J., and Steitz, T. A. (2001) Structure of the replicating complex of a pol α family DNA polymerase, *Cell 105*, 657−667.
33. Liu, S., Knafles, J. D., Chang, J. S., Waszak, G. A., Baldwin, E. T., Deibel, M. R., Jr., Thomsen, D. R., Homa, F. L., Wells, P. A., Tory, M. C., Poorman, R. A., Gao, H., Qiu, X., and Seddon, A. P. (2006) Crystal structure of the herpes simplex 1 virus DNA polymerase, *J. Biol. Chem.* (in press).
34. Wang, T. S., Wong, S. W., and Korn, D. (1989) Human DNA polymerase α: Predicted functional domains and relationships with viral DNA polymerases, *FASEB J. 3*, 14−21.
35. Wang, J., Sattar, A. K., Wang, C. C., Karam, J. D., Konigsberg, W. H., and Steitz, T. A. (1997) Crystal structure of a pol α family replication DNA polymerase from bacteriophage RB69, *Cell 89*, 1087−1099.
36. Mercozzi, S., West, A. P. J., and Dougherty, D. A. (1996) Cation interactions in aromatics of biological and medicinal interest: Electrostatic potential surfaces as a useful qualitative guide, *Proc. Natl. Acad. Sci. U.S.A. 93*, 10566−10571.
37. Yang, G., Wang, J., and Konigsberg, W. (2005) Base Selectivity is Impaired by Mutants that Perturb Hydrogen Bonding Networks in the RB69 DNA Polymerase Active Site, *Biochemistry 44*, 3338−3346.
38. Mendelman, L. V., Petruska, J., and Goodman, M. F. (1990) Base mispair extension kinetics. Comparison of DNA polymerase α and reverse transcriptase, *J. Biol. Chem. 265*, 2338−2346.
39. Perrino, F. W., and Loeb, L. A. (1989) Differential extension of 3′ mispairs is a major contribution to the high fidelity of calf thymus DNA polymerase-α, *J. Biol. Chem. 264*, 2898−2905.
40. Kool, E. T., Morales, J. C., and Guckian, K. M. (2000) Mimicking the Structure and Function of DNA: Insights into DNA Stability and Replication, *Angew. Chem., Int. Ed. 39*, 990−1009.
41. Kool, E. T. (2002) Active site tightness and substrate fit in DNA replication, *Annu. Rev. Biochem. 71*, 191−219.
42. Sintim, H. O., and Kool, E. T. (2006) Remarkable sensitivity to DNA base shape in the DNA polymerase active site, *Angew. Chem., Int. Ed. 45*, 1974−1979.
43. Ogawa, A. K., Wu, Y., McMinn, D. L., Liu, J., Schultz, P. G., and Romesberg, F. E. (2000) Efforts toward the Expansion of the Genetic Alphabet: Information Storage and Replication with Unnatural Hydrophobic Base Pairs, *J. Am. Chem. Soc. 122*, 3274−3287.
44. Berger, M., Wu, Y., Ogawa, A. K., McMinn, D. L., Schultz, P. G., and Romesberg, F. E. (2000) Universal bases for hybridization, replication and chain termination, *Nucleic Acids Res. 28*, 2911−2914.
45. Wu, Y., Ogawa, A. K., Berger, M., McMinn, D. L., Schultz, P. G., and Romeberg, F. E. (2000) Efforts toward Expansion of the Genetic Alphabet: Optimization of Interbase Hydrophobic Interactions, *J. Am. Chem. Soc. 122*, 7621−7632.
46. Ogawa, A. K., Wu, Y., Berger, M., Schultz, P. G., and Romeberg, F. E. (2000) Rational Design of an Unnatural Base Pair with Increased Kinetic Selectivity, *J. Am. Chem. Soc. 122*, 8803−8804.
47. Hendrickson, C. L., Devine, K. G., and Benner, S. A. (2004) Probing minor groove recognition contacts by DNA polymerases and reverse transcriptases using 3-deaza-2′-deoxyadenosine, *Nucleic Acids Res. 32*, 2241−2250.

BI061243S